HIERARCHICAL STRUCTURE INVESTIGATIONS OF BIOGENIC FERRIHYDRITE SAMPLES

M. BALASOIU[1,4], S.V. STOLYAR[2,6], R.S. ISKHAKOV[2,6], L.A. ISHCHENKO[2], YU.L. RAIKHER[3], A.I. KUKLIN[4], O.L. ORELOVICH[4], YU.S. KOVALEV[4], T.S. KURKIN[5], G.M. ARZUMANIAN[4]

[1]Horia Hulubei National Institute of Physics and Nuclear Engineering, P.O. Box MG-6, Bucharest-Magurele, Romania
E-mail: balasoiumaria@yahoo.com
[2]Siberian Federal University, 660041, Krasnoyarsk, Russia
E-mail: rauf@iph.krasn.ru
[3]Institute of Continuum Media Mechanics, Ural Branch of RAS, 614013, Perm, Russia
E-mail: raikher@icmm.ru
[4]Joint Institute of Nuclear Research, Dubna, 141980, Russia
E-mail: kuklin@nf.jinr.ru
[5]Institute of Synthetic Polymer Materials RAS, Moscow, 117393, Russia
[6]Institute of Physics, Siberian Branch of RAS, 660036, Krasnoyarsk, Russia

Received September 5, 2009

Results of observation and preliminary analysis on morphology and structure of ferrihydrite particles produced *in vivo* by *Klebsiella oxytoca* bacteria are presented. In particular, optical microscopy, scanning electron microscopy and small angle X-ray scattering in accordance with one another point out the fractal structure of the biomineral particle surface. The effect of the bacteria age (the duration of growth) on the fractal dimension is established and characterized.

Key words: ferrihydrite nanoparticles, Klebsiella oxytoca bacteria, optical microscopy, SEM, SAXS.

1. INTRODUCTION

Ferrihydrite, an iron oxide hydroxide, is a much widespread material [1–9]. It enters, as a constituent, in various bands of environments, such as clays and soils, soluble fraction of weathered rocks, ground and hydrothermal spring waters, etc. Of all the types of iron oxides, ferrihydrite has a largest distribution in living organisms, where it is found in the form of ferritin, an iron storage protein. Moreover, ferrihydrite is found to be present in some microbial communities, where it is produced by bacteria as a result of their metabolism [1–4]. In addition to this, ferrihydrite has been found in several extraterrestrial materials, as meteorites and interplanetary dust particles [1].

Ferrihydrite, being an antiferromagnetic oxyhydroxide in the bulk, in nanophase state yields the particles which possess permanent magnetic moments. The latter originate from the loss of compensation in a finite spin assembly of a particle where the number of surface spins is by no means negligible in comparison with that in the bulk. The two most known forms of these magnetic ferrihydrite particles are distinguished with respect to the number of lines in their respective X-ray diffraction patterns [5–7]. Accordingly varies the nanocrystal size: from 2–4 nm in 2-line modification to 5–6 nm in 6-line modification. The 6-line ferrihydrite was identified as a mineral by International Mineralogical Association (IMA) in 1973 [8,9]. The less crystalline 2-line ferrihydrite, on the other hand, is not believed to be a mineral. In comparison with most minerals, both 2-line and 6-line ferrihydrites show very broad diffraction lines that makes it difficult to extract accurate structural information.

With its high specific surface area [10], ferrihydrite is a very reactive substance. It can interact, either by surface adsorption or by co-precipitation, with a number of environmentally important chemical species, including arsenic, heavy metals e.g. lead or mercury, with phosphates and many organic molecules. Thermodynamically, ferrihydrite is a metastable form of iron oxide and is known to be a precursor for more crystalline minerals like hematite and goethite [11]. Importance of ferrihydrite in the environmental iron cycle and in metallurgy processes was for a long time the issue of main interest on the part of the scientific community. Recently, the magnetic susceptibility of the ferrihydrite particles enhanced by the superantiferromagnetism effect, together with the presence of magnetic moment independent on the external field were recognized as possibility of magnetic manipulation upon these natural objects [12, 13] opening the way of their in nanomedicine and biotechnologies [14].

In the present paper samples containing biogenic ferrihydrite nanoparticles produced by bacteria *Klebsiella oxytoca* are investigated. We note that biogenic minerals often turn out to be in fact composites where nano- or micro-scale amorphous or crystalline materials are densely mixed with organic molecules. Due to that, complex hierarchical structures from nanometer to the macroscopic scale are formed. The mechanisms of biomineral formation are not fully understood, and while they are of interest in their own right yielding new insights into the genetic control of biological structure [15], they may also provide new concepts for artificial structures and inspire solutions in design and engineering of nanoscale materials.

2. EXPERIMENTAL RESULTS

As a result of variation of the growth conditions for the microorganisms (growth period, light exposition, potassium citrate – ferric citrate rate, etc.),

bacterium *Klebsiella oxytoca* creates, as was established in previous works [2–4,12,13], two types of ferrihydrite nanoparticles whose differences are accurately identified by means of Mössbauer spectroscopy [2–4] and static magnetic measurements analysis [12,13]. Samples Fe12 and Fe34 have been separated from a bacterial biomass grown during 8 and 21 days, respectively.

In the present study the morphology and structure of these two ferrihydrite samples produced by *Klebsiella oxytoca* are investigated by means of a number of procedures at different length scales: optical microscopy with magnification $\times 10^2$ (Fig. 1); scanning electron microscopy with equivalent magnification $\times 4 \cdot 10^4$ (Figs. 2 and 4), and small angle X-ray scattering with resolution $\times 10^8$ (Figs. 3). Under the optical microscope (Microscope type Leica DM IRB), sample Fe12 looks as a polycrystalline object (Fig. 1a) while Fe34 displays a sponge-like texture (Fig. 1b).

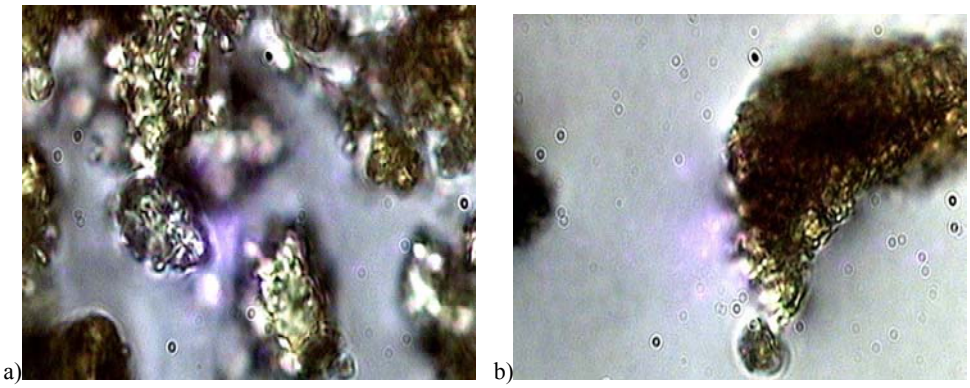

a) b)

Fig. 1 – Optical micrograph of sample Fe12 (a) and sample Fe34 (b).

In Fig. 2 the same samples under a JEOL type JSM-840 scanning electron microscope (SEM) are presented.

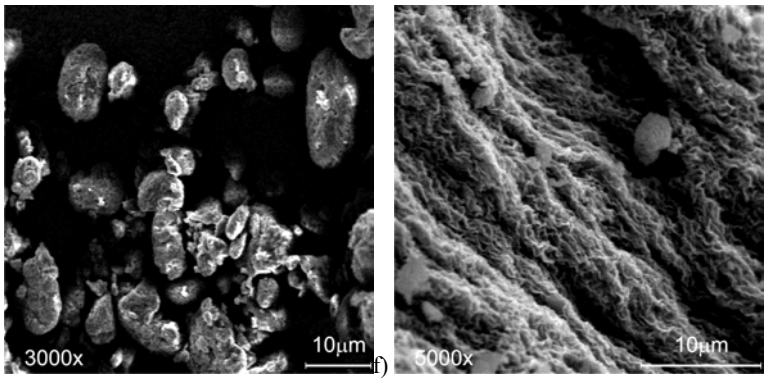

a) f)

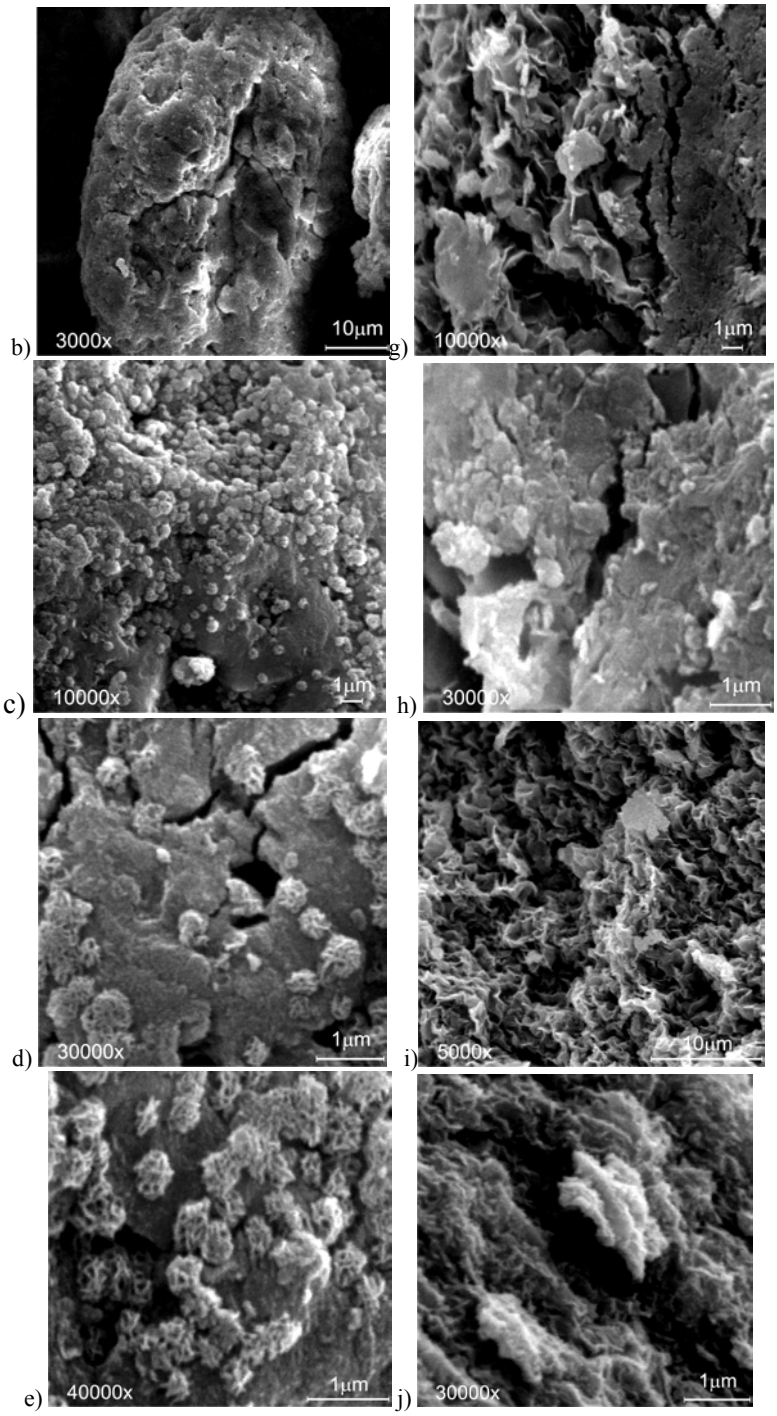

Fig. 2 – SEM images of two samples containing ferrihydrite nanoparticles obtained by means of two different methods; sample Fe12 (a–e) and sample Fe34 (f–j).

The SEM images reveal structural differences between the samples. Sample Fe12 has a grain texture (Fig. 2a), in Fig. 2b the enlarged image of one grain is given. With a higher instrument resolution, in Fig. 2c small entities on the grain surface are distinguished. Upon further enhancement of resolution, these entities appear as multi-lateral particles or clusters of smaller objects. Sample Fe34 has a stratified and friable branched texture, see Figs. 2f–j. The samples were also studied by small angle X-ray (SAXS) method on Brucker Nanostar instrument available at the Institute of Synthetic Polymer Materials RAS, Moscow. The experimental setup used covers the Q range of 0.01–0.11 $Å^{-1}$. In Fig. 3 experimental and fitting curves are presented.

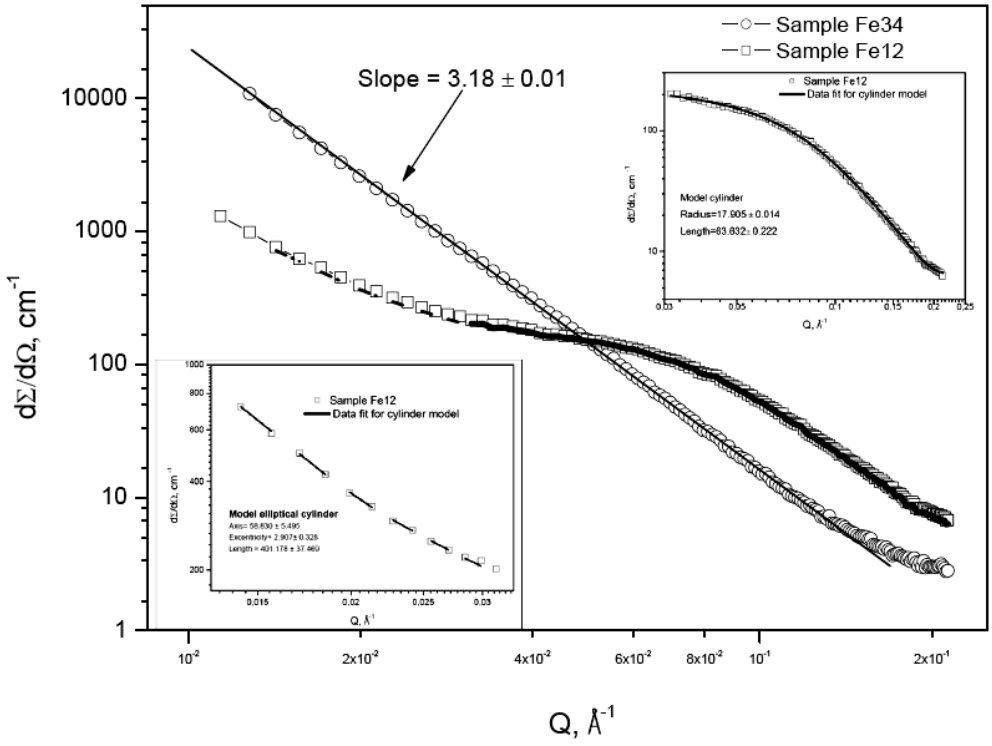

Fig. 3 –Small angle X-ray scattering experimental curves from samples Fe12 and Fe34 obtained at Brucker Nanostar SAXS spectrometer at the Institute of Synthetic Polymer Materials RAS, Moscow.

3. DATA ANALYSIS AND COMMENTS

Using the FITTER program [16] to model experimental data, it was found that a form factor for a round cylinder [17] having the radius R and length H:

$$P(Q) = A\int_0^1 \Lambda_1^2(QR\sqrt{1-x^2})S^2(QHx/2)dx + B\,, \quad (1)$$

where,

$\Lambda_1(t) = 2J_1(t)/t$;

$S(t) = \sin t/t$;

J_1 is the cylindrical Bessel function of order 1,

best describes the scattering signal from Sample Fe12 in the analyzed Q range of 0.03 ÷ 0.25 Å^{-1}.

In the Q range of 0.013 ÷ 0.03 Å^{-1}, the form factor for elliptical cylinder [17] with half-axes a, v and length H:

$$P(Q) = A\int_0^1 \Psi_{EC}(Q, a\sqrt{1-x^2})S^2(QHx/2)dx + B\,, \quad (2)$$

where,

$$\Psi_{EC}(Q,a) = \frac{1}{\pi}\int_0^{\pi} \Lambda_1^2\left(Qa\sqrt{\frac{1+v^2}{2} + \frac{1-v^2}{2}\cos y}\right)dy\,,$$

was found to best fit the region of experimental curve.

Specific to sample Fe12 at a micron scale (see Fig. 2e) is the presence of some formations composed from "sockets" separated by "edges". From SEM image is evident that they are randomly oriented. This fact allows ignoring the structure factor of the system, and just taking the form factor.

The experimental curve obtained from sample Fe34 reveals in the Q range of 0.01 ÷ 0.11 Å^{-1} a power-law behavior: $I(Q) \approx Q^{-\alpha}$, with the exponent $\alpha = 3.18 \pm 0.01$. This indicates that the system has a fractal structure. When $3 < \alpha < 4$, the scattering objects are considered to be surface fractals which fractal dimension is given by formula $D_S = 6 - \alpha$ [18]. Consequently, for sample Fe34, the system structure is characterized by the fractal dimension $D_S = 2.82 \pm 0.01$ specific to highly branched surface fractals.

In the case of sample Fe12, by SAXS data analysis several dimensional levels are detected (see Fig. 3). At the first dimensional level, cylindrical structural entities of radius R=17.9 Å ± 0.02 Å and length, H=63.6 Å ± 0.2 Å are obtained. Next level is found to be characterized by elliptical cylinder formations with axis a = 58.8 Å ± 5.5 Å, length H = 401.2 Å ± 37.5 Å and eccentricity e = 2.9 Å ± 0.3 Å. These results agree with the evidence from SEM images.

4. CONCLUSIONS

As follows from our results, SAXS technique proves its ability to reliably discriminate several types of structural peculiarities of the bacterial ferrihydrite

phases. This is important because these phases differ in magnetic, *i.e.* most essential for nanomedicine, properties. For further investigations of bacterial ferrihydrite structural phases, small angle neutron scattering with contrast variation is required [19], while for magnetic microstructure differentiation experiments with polarized neutrons are needed [20, 21].

Acknowledgements. The work was accomplished with the financial support of Grant 224/11.04.2008 of Romanian Governmental Plenipotentiary at JINR.

REFERENCES

1. G. Matrajt and D. Blanot, *Properties of synthetic ferrihydrite as an amino acid adsorbent and a promoter of peptide bond formation*, Amino Acids **26**, 153–158(2004).
2. S.V. Stolyar, O.A. Bayukov, Yu.L. Gurevich *et al*., *Iron-containing nanoparticles from microbial metabolism*, Inorganic Materials **42** (2006), 763–768.
3. S.V. Stolyar, O.A. Bayukov, Yu.L. Gurevich *et al*., *Mössbauer study of bacterial ferrihydrite*, Inorganic Materials **43** (2007)638–641.
4. S.V. Stolyar, O.A. Bayukov, V.P. Ladygina *et al*., *Mössbauer investigations of temperature transformations in bacterial ferrihydrite*, Physics of Solid State (2010) – submitted.
5. D.E. Janney, J.M. Cowley, and P.R. Buseck, *Transmission electron microscopy of synthetic 2- and 6-line ferrihydrite*, Clays and Clay Minerals **48** (2000), 111–119.
6. D.E. Janney, J.M. Cowley and P.R. Buseck, *Structure of synthetic 2-line ferrihydrite by electron nanodiffraction*, American Mineralogist **85** (2000), 1180–1187.
7. D.E. Janney, J.M. Cowley, and P.R. Buseck, *Structure of synthetic 6-line ferrihydrite by electron nanodiffraction*, American Mineralogist **86** (2001), 327–335.
8. F.V. Chuckrov, B.B. Zvyagin, A.I. Gorshov *et al*., *Ferrihydrite* International Geology Review **16** (1973), 1131–1143.
9. M. Fleischer, G.Y. Chao, and A. Kato, *New mineral names*, American Mineralogist **60** (1975), 485–489.
10. R. Skomski, *Nanomagnetics*, J. Phys.: Condens. Matter **15** (2003), R841–R896.
11. H. Stanjek and P.G. Weidler, *The Effect of Dry Heating on the Chemistry, Surface Area, and Oxalate Solubility of Synthetic 2-Line and 6-Line Ferrihydrite,* Clay minerals **27** (1992), 397–412.
12. Yu.L. Raikher and V.I. Stepanov, *Magnetic relaxation in a suspension of antiferromagnetic nanoparticles*, JETP, **107**, 3 (2008) 435–444.
13. Yu.L. Raikher, V.I. Stepanov, S.V. Stolyar *et al*., *Magnetic properties of biomineral nanoparticles produced by Klebsiella oxytoca bacteria,* Physics of the Solid State (2010) – to appear; JINR Preprint P19-2009–112 (Russ.)
14. S.V. Stolyar, R.S. Iskhakov, V.P. Ladygina *et al*., *Magnetic nanoparticles for medical applications,* Proc. International Conference NMMM-21, Moscow, MSU, 28 June–4 July (2009), 405 (Russ.)
15. P.U.P.A. Gilbert, M. Abrecht, B. Frazer, *The organic-mineral interface in biominerals*, Rev. Mineralogy & Geochemistry **59** (2005), 157–185.
16. A.G. Soloviov, A.V. Stadnik, A.H. Islamov, A.I. Kuklin, *FITTER. The package for fitting a chosen theoretical multi-parameter function through a set of data points. Application to experimental data of the YuMO spectrometer. Version 2.1.0. Long Write-up and User's Guide*, JINR Communications E10-2008-2, http://www.jinr.ru/programs/jinrlib/fitter/indexe.html
17. L.A. Feigin and D.I. Svergun, *Structure Analysis by Small-Angle X-Ray and Neutron Scattering,* 1987 Plenum Press New York.

18. H.D. Bale and P.W. Schmidt, *Small-angle X-ray scattering investigations of submicroscopic porosity with fractal properties,* Phys.Rev.Lett. **53**, 6 (1984), 596–599.
19. B. Grabcev, M. Balasoiu, A.Tarziu *et al., Application of contrast variation method in SANS experiments with ferrofluids,* J. Mag. Mag. Mater., 201(**1999**), 140–143.
20. S.M. Yusuf, J.M. De Teresa, M.D. Mukadam *et al*., *Experimental study of the structural and magnetic properties of γ-Fe_2O_3 nanoparticles,* Phys. Rev. B **74** (2008), 224428(11).
21. M. Balasoiu and V.L. Aksenov, *Neutron depolarization and mSR studies of ferrofluids,* J. Optoelectronics and Adv. Mater. **10,** 12 (2008), 3322–3327.